Atomistic Study of Crack-Tip Cleavage to Dislocation Emission Transition in Silicon Single Crystals

Dipanjan Sen,[1,2] Christian Thaulow,[2,3] Stella V. Schieffer,[2] Alan Cohen,[2,4] and Markus J. Buehler[2,*]

[1]*Department of Materials Science and Engineering, Massachusetts Institute of Technology, 77 Massachusetts Avenue, Cambridge, Massachusetts 02139, USA*

[2]*Laboratory for Atomistic and Molecular Mechanics, Department of Civil and Environmental Engineering, Massachusetts Institute of Technology, 77 Massachusetts Avenue, Room 1-235A&B, Cambridge, Massachusetts 02139, USA*

[3]*Department of Engineering Design and Materials, The Norwegian University of Science and Technology, NO-7491 Trondheim, Norway*

[4]*Department of Mechanical Engineering, Massachusetts Institute of Technology, 77 Massachusetts Avenue, Cambridge, Massachusetts 02139, USA*

(Received 7 February 2010; published 11 June 2010)

At low temperatures silicon is a brittle material that shatters catastrophically, whereas at elevated temperatures, the behavior of silicon changes drastically over a narrow temperature range and suddenly becomes ductile. This brittle-to-ductile transition has been observed in experimental studies, yet its fundamental mechanisms remain unknown. Here we report an atomistic-level study of a fundamental event in this transition, the change from brittle cleavage fracture to dislocation emission at crack tips, using the first principles based reactive force field. By solely raising the temperature, we observe an abrupt change from brittle cracking to dislocation emission from a crack within a ≈10 K temperature interval.

DOI: 10.1103/PhysRevLett.104.235502 PACS numbers: 62.25.Mn, 46.50.+a, 62.20.fk

The mechanical response of solids subject to extreme stress is controlled by atomistic mechanisms near stress concentrations such as crack tips [Fig. 1(a)] [1–4]. It has been shown experimentally that key mechanisms are controlled by the temperature, where low temperatures tend to lead to a more brittle and higher temperature to a more ductile material behavior [5–7]. In silicon, studies of single dislocation-free crystals with a crack have revealed that the material response changes from brittle-to-ductile as the temperature is increased [6,8,9]. This brittle-to-ductile transition (BDT) is extremely sharp and occurs within a few degrees in temperature variation [9]. The importance of dislocation nucleation events at the crack tip to BDT has been shown experimentally, and is known to affect both the BDT temperature [10] and its sensitivity to the strain rate [11]. What remains missing is an atomistic picture of events at a crack tip that occur under changes of the temperature [12], which is crucial to eventually understanding the sudden change from purely brittle-to-ductile material behavior.

The development of atomistic-level understanding of crack-tip events in silicon with increasing temperature have been hindered partly due to the lack of atomistic models that enable the simulation of sufficiently large systems to accurately describe the fracture processes at a range of temperatures. Describing bond breaking processes in silicon requires quantum mechanical (QM) methods to properly describe the complex electronic rearrangements, where large changes in bond angles and coordination can severely affect the interatomic forces [13–15]. Yet, accurate QM studies for large system sizes remain impracticable. An alternative approach has been to use relatively simple empirical relationships between bond stretch and force [16,17], but earlier results have suggested that fracture in silicon cannot be modeled with such force fields [13].

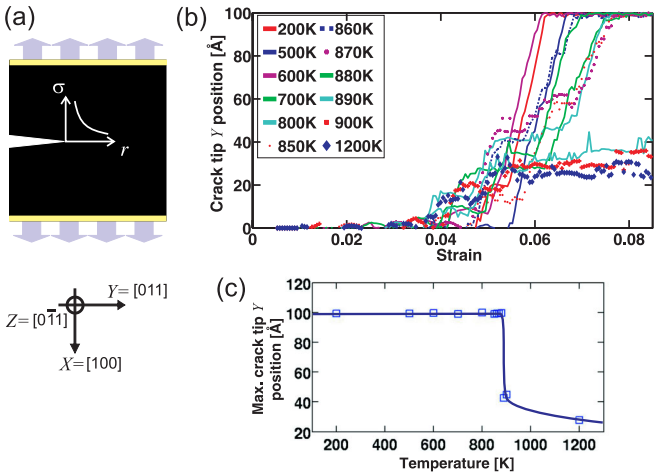

FIG. 1 (color online). System geometry and crack dynamics analysis. (a) Silicon single crystal under mode I loading with {100}⟨110⟩ edge crack. (b) Crack-tip position for a range of temperatures from 200 to 1200 K, as a function of strain. At low temperatures the crack reaches an equilibrium speed of about 2500 m/s, whereas for temperatures above 890 K, the crack comes to a stop at around 6% strain. (c) Analysis of the maximum Y position of the crack at the end of the simulation, as a function of temperature. A dramatic, sudden change is seen in the small temperature interval between 880–890 K, where the crack stops in the middle of the sample.

Here we apply the first principles based reactive force field (ReaxFF), which retains nearly the accuracy of QM, even for bond breaking events. The ReaxFF parameters are determined solely by fitting to QM data on silicon [18]. Earlier studies with ReaxFF have shown that it reproduces key experimental observations of fracture of silicon [14,15]. Material properties calculated based on the ReaxFF silicon potential, including elastic properties, fracture surface energy and dislocation properties agree well with experimental and first principles results [14,15]. Extending earlier studies, we calculate the generalized stacking fault energy curve for slip in the [112] direction on the (111) plane and find an unstable stacking fault energy $\gamma_{\mathrm{US}} = 0.16\ \mathrm{eV/\AA^2}$, in close agreement with density functional theory predictions of $0.13\ \mathrm{eV/\AA^2}$ [19]. We use a parallelized implementation of ReaxFF (GRASP) to perform large-scale molecular dynamics simulations [20].

Figure 1(a) depicts the three-dimensional molecular dynamics model [21,22] with a surface crack under mode I tensile loading. We consider a crystal with an initial crack serving as failure initiation point. The crystal is oriented so that the X-Y-Z directions are $(100) \times (011) \times (0\bar{1}1)$, creating a (100) fracture plane with initial [011] fracture direction. Our choice of the {100} crack plane orientation is motivated by our desire to create a model system in which the competition between brittle crack extension and dislocation nucleation can be studied under mode I loading. Specifically, the geometry considered here features the possibility for brittle crack extension (close to the maximum tensile or crack-opening hoop stress around a mode I crack), and a glide plane inclined by 54.7° to the cleavage plane (close to the maximum shear stress around a mode I crack at ≈70°). Other crystal or crack orientations do not have this feature (e.g., the {111} or {110} crack planes under mode I loading result in different planes for crack propagation and dislocation nucleation, with different Schmidt factors).

The thickness of the systems is ≈15 Å, and the system consists of approximately 27 500 atoms (ReaxFF is 1–2 orders of magnitude more expensive than conventional force fields). Unlike in earlier studies (where a hybrid simulation approach was used that combined a ReaxFF with a Tersoff potential) [14,15] the entire domain is modeled using ReaxFF. The system size is $196\ \text{Å} \times 184\ \text{Å} \times 15\ \text{Å}$ with periodic boundary conditions in X and Z directions, with initial crack length 40 Å (one fifth of the sample size in the Y direction). Additional simulations with much larger system sizes have been carried out, and similar results as reported here are observed (in thicker systems we observe the nucleation of dislocation loops at the crack tip). We simulate a canonical ensemble (NVT) with temperature control using a Berendsen thermostat [23]. To apply load, we continuously strain the system under mode I tensile load, by displacing the boundaries [16] at a strain rate of $1 \times 10^9\ \mathrm{s^{-1}}$. The crack-tip position is determined by finding the surface atom with maximum Y position in the interior of a search region inside the slab. Velocities of the crack tip are calculated by averaging the time derivative of the crack-tip position. Visualizations are performed using the Visual Molecular Dynamics software [24].

We carry out twelve computational experiments at temperatures from 200 to 1200 K, with exactly the same initial and boundary conditions (other than temperature). Figure 1(b) shows the results of the crack-tip position over time for all temperatures. We find that the results fall in two types of behavior, and that there exists a sudden change in the behavior as the temperature is increased beyond a critical temperature. At the lowest temperatures (200 to 500 K) the system behaves in a perfectly brittle fashion where the crack propagates in steps along the usual {111} fracture surface, as known from experiment and other simulations. The crack speed quickly approaches $2\text{–}3\ \mathrm{km \cdot s^{-1}}$ after fracture initiation, in agreement with earlier work [13,15] and experiment [25]. To test the applicability of the Griffith criterion for brittle fracture, the critical stress intensity factor K_{Ic} is calculated from the simulations to be $\approx 0.83\ \mathrm{MPa}\sqrt{\mathrm{m}}$ (500 K). Based on the surface energy the Griffith fracture toughness is $0.82\ \mathrm{MPa}\sqrt{\mathrm{m}}$, in good agreement.

From Fig. 1(b) it can be seen that as the temperature is increased up to 800 K, small steps of crack arrest occur along the crack pathway (here, crack arrest refers to a complete stop of crack motion for a few picoseconds) followed by reinitiation of the crack. The overall crack path is brittle, without occurrence of dislocations. As the temperature is increased further beyond 800 K, the crack arrest and reinitiation behavior gradually becomes more evident and features larger arrest times, until suddenly, at a critical temperature of about 890 K, the crack comes to a complete stop in the middle of the sample, without any further crack propagation [Figs. 1(b) and 1(c)].

The analysis of the atomistic structure during crack extension through a slip vector analysis [26] explains this observation. We consider two representative cases from either side of the critical temperature. Figure 2(a) displays snapshots of crack dynamics at 200 K, showing ''clean'' brittle fracture through generation of almost perfectly flat atomic surfaces. The analysis at 1200 K shown in Fig. 2(b) reveals the nucleation of a partial dislocation from the crack tip. Once a 90° partial dislocation is emitted on a $\{\bar{1}11\}$ glide plane the crack stops. We find that the slip direction is [211] and the slip vector is 2.3 Å, in good accordance with the partial Burgers vector on that glide plane. These results reveal a very sharp transition from brittle cleavage fracture to dislocation emission behavior within an extremely narrow temperature regime of ≈10 K.

The mechanism for the transition from the cleavage fracture to dislocation emission behavior can be explained based on atomic mechanisms at the crack tip. Figures 3(a)

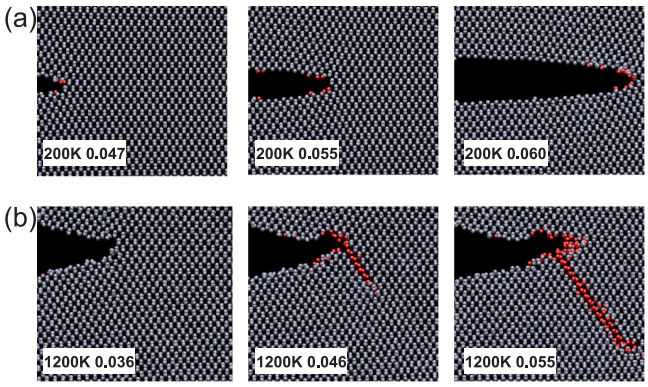

FIG. 2 (color online). Atomistic-level crack mechanisms at 200 K (a) and 1200 K (b). Atoms are colored according to a slip vector analysis [slipped atoms are shown darker (in red online)]. (a) Brittle cleavage fracture under creation of smooth fracture surfaces is observed. (b) Slight crack opening is followed by sudden crack blunting, with emission of a dislocation.

and 3(b) show the brittle fracture process (200 K), which proceeds through small fracture steps (nanocracks) on {111} planes. These nanocracks, consisting of single bond breaking events on alternating {111} planes intersecting at the crack tip, enable the brittle crack to effectively move forward in the ⟨011⟩ direction. In the brittle regime, for any crack extension there is a competition between the energetically less favorable {100} plane, which has a higher surface energy, and the {111} planes, which intersect at 54.7° with respect to the {100} plane. The tensile stresses that act on the {100} plane are decisive for the crack to remain on this plane. Nevertheless, crack-tip crack propagation along the {111} planes takes place locally, in agreement with earlier findings that have suggested that the {111} is a preferred fracture plane [27].

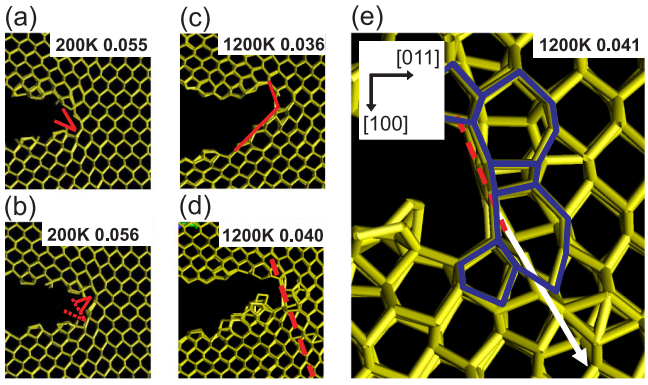

FIG. 3 (color online). Crack-tip mechanisms at 200 and 1200 K. (a) and (b) Brittle fracture at 200 K, with small fracture steps on {111} planes (nanocracks). These nanocracks facilitate brittle crack motion in the effective ⟨100⟩ direction. (c) Ledge formed at 1200 K, where the crack has diverted along a {111} cleavage plane. (d) Formation of a 5-7-4-7-5 ring, reflecting a disordered zone formation. (e) Detailed structure of the disordered zone and first indication of emission of a dislocation at 1200 K. The arrow is aligned with the $(\bar{1}11)$ glide plane and shows the direction of dislocation movement.

As the critical temperature is approached, crack-tip blunting dominates and is accompanied by changes in the perfect hexagonal ring structure at the crack tip. Bond rotations at the crack tip lead to the formation of new covalent bond structures that differ from the typical 6-membered hexagonal rings. These less structured, disordered zones extend over ≈10 Å. Figures 3(c)–3(e) show a detailed analysis at 1200 K where a ledge has formed and the crack has diverted along a {111} cleavage plane.

The emergence of these structural changes at the crack tip has major implications on the behavior of the crack. As the crack tip becomes wider, the stress required for brittle fracture increases, because of the lowering of the crack-opening stress intensity at a blunt tip [15,28]. Moreover, blunting induces a change of the crack-tip shape, as it facilitates a rotation of the crack front to align with {111} planes, leading to the formation of a small {111} cleavage ledge at the crack tip. At the ledge tip, the loading now exhibits mode II shear components oriented at approximately 55° with respect to the {100} plane. It has been shown theoretically that even very small amounts of shear loading (≈10% of tensile load) can lead to emission of dislocations [29]. This suggests that the change of the stress field due to ledges formation may indeed induce the nucleation of dislocations. Notably, in contrast to experimental observations of the presence of ledges *after* the generation of dislocations [10,30], or ledges due to surface irregularities caused by river patterns, microstructural or impurity distribution variations, the ledges observed in our study are intrinsically formed by the crack-tip blunting and rotation mechanisms, prior to any dislocation nucleation. The mechanism is summarized in Fig. 4.

Our results provide an atomistic-scale view of changes in crack-tip mechanisms from cleavage fracture to dislocation emission in silicon under changes in the temperature. Our fully atomistic approach offers insight to crack-tip mechanisms that is currently missing from theoretical analyses of dislocation emission [31–34]. Our simulations reproduce the typical sudden change of key crack-tip mechanisms under slight temperature variations. However, while our study may have revealed one possible mechanism associated with the BDT, more studies need to be carried out to probe the behavior of the system under strain rate variations. This is critical to make a rigorous link to BDT mechanisms seen in experiment, which are performed at lower rates.

Moreover, our analysis focused solely on events at a single crack tip, and on mechanisms associated with crack extension or dislocation nucleation and thus does not yet capture the full complexity of the BDT. Still, the mechanisms obtained from this work could be combined with continuum dislocation mobility models using a coupled multiscale modeling approach to study the whole process

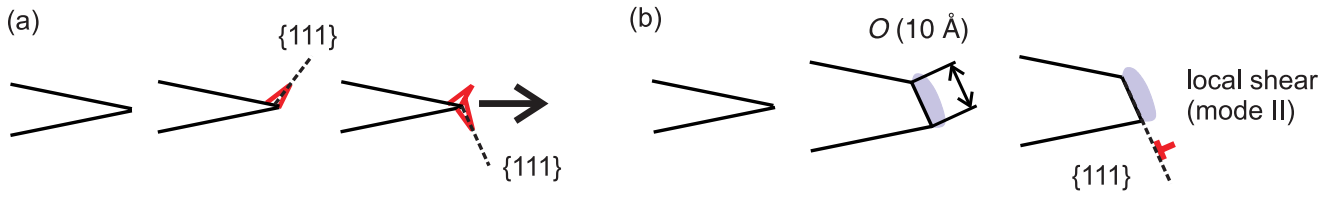

FIG. 4 (color online). Mechanisms associated with brittle crack extension and dislocation nucleation, here visualized in a schematic representation for low and high temperatures. (a) [low T], Zigzag mechanism of brittle cracking via the formation of nanocracks on the {111} plane. (b) [high T], Formation of a disordered zone that blunts the crack-tip and thereby creates a crack-tip ledge (dislocation emitted along the ledge direction).

BDT over a broad entire range of temperatures, strain rates, and length scales. Reaction pathway analyses [35–37] of formation of disordered zones and ledges uncovered in this study could be undertaken in order to obtain activation energy barriers for these events. This information, combined with critical dislocation loop nucleation barriers [38] under the influence of crack-tip ledges and disordered zones, could provide quantitative energetics required to simulate dislocation nucleation events in large-scale models.

We acknowledge fruitful discussions with A. S. Argon and S. Yip (MIT). We are also grateful for discussions with W. A. Goddard (Caltech) and A. Van Duin (Penn State) on ReaxFF modeling. We thank A. Thompson (Sandia National Laboratory) for providing us with the GRASP molecular simulation code.

*Corresponding author.
mbuehler@MIT.EDU

[1] L. B. Freund, *Dynamic Fracture Mechanics* (Cambridge University Press, Cambridge, England, 1990).
[2] K. B. Broberg, *Cracks and Fracture* (Academic Press, San Diego, 1999).
[3] J. P. Hirth and J. Lothe, *Theory of Dislocations* (Wiley-Interscience, New York, 1982).
[4] J. R. Kermode *et al.*, Nature (London) **455**, 1224 (2008).
[5] P. Gumbsch *et al.*, Science **282**, 1293 (1998).
[6] P. D. Warren, Scr. Metall. **23**, 637 (1989).
[7] A. S. Balankin and A. D. Izotov, Rev. Mex. Fis. **41**, 783 (1995).
[8] C. S. John, Philos. Mag. **32**, 1193 (1975).
[9] J. Samuels and S. G. Roberts, Proc. R. Soc. A **421**, 1 (1989).
[10] A. George and G. Michot, Mater. Sci. Eng. **164**, 118 (1993).
[11] C. Scandian *et al.*, Phys. Status Solidi (a) **171**, 67 (1999).
[12] J. Li, A. H. W. Ngan, and P. Gumbsch, Acta Mater. **51**, 5711 (2003).
[13] N. Bernstein and D. W. Hess, Phys. Rev. Lett. **91**, 025501 (2003).
[14] M. J. Buehler, A. C. T. van Duin, and W. A. Goddard, Phys. Rev. Lett. **96**, 095505 (2006).
[15] M. J. Buehler *et al.*, Phys. Rev. Lett. **99**, 165502 (2007).
[16] M. J. Buehler and H. Gao, Nature (London) **439**, 307 (2006).
[17] D. Holland and M. Marder, Phys. Rev. Lett. **80**, 746 (1998).
[18] A. C. T. v. Duin *et al.*, J. Phys. Chem. A **107**, 3803 (2003).
[19] Y. M. Juan and E. Kaxiras, Philos. Mag. A **74**, 1367 (1996).
[20] D. Sen, A. Cohen, A. Thompson, A. C. T. van Duin, W. A. Goddard, and M. J. Buehler, in *Integrated Miniaturized Materials—From Self-Assembly to Device Integration*, edited by C. J. Martinez *et al.*, MRS Symposia Proceedings No. 1272 (Materials Research Society, Warrendale, PA, 2010).
[21] M. P. Allen and D. J. Tildesley, *Computer Simulation of Liquids* (Oxford University Press, New York, 1989).
[22] M. J. Buehler, *Atomistic Modeling of Materials Failure* (Springer, New York, 2008).
[23] H. J. C. Berendsen *et al.*, J. Chem. Phys. **81**, 3684 (1984).
[24] W. Humphrey, A. Dalke, and K. Schulten, J. Mol. Graphics **14**, 33 (1996).
[25] J. A. Hauch *et al.*, Phys. Rev. Lett. **82**, 3823 (1999).
[26] J. A. Zimmerman *et al.*, Phys. Rev. Lett. **87**, 165507 (2001).
[27] R. Perez and P. Gumbsch, Phys. Rev. Lett. **84**, 5347 (2000).
[28] J. Schiotz, L. M. Canel, and A. E. Carlsson, Phys. Rev. B **55**, 6211 (1997).
[29] J. R. Rice and G. B. Beltz, J. Mech. Phys. Solids **42**, 333 (1994).
[30] A. S. Argon and B. J. Gally, Scr. Mater. **45**, 1287 (2001).
[31] J. R. Rice, J. Mech. Phys. Solids **40**, 239 (1992).
[32] S. J. Zhou and R. Thomson, J. Mater. Res. **6**, 639 (1991).
[33] G. Xu, A. S. Argon, and M. Ortiz, Philos. Mag. A **75**, 341 (1997).
[34] G. P. Cherepanov, Appl. Mech. Rev. **47**, S326 (1994).
[35] G. Henkelman, B. P. Uberuaga, and H. Jónsson, J. Chem. Phys. **113**, 9901 (2000).
[36] D. H. Warner, W. A. Curtin, and S. Qu, Nature Mater. **6**, 1004 (2007).
[37] M. de Koning *et al.*, Phys. Rev. B **58**, 12555 (1998).
[38] T. Zhu, J. Li, and S. Yip, Phys. Rev. Lett. **93**, 025503 (2004).